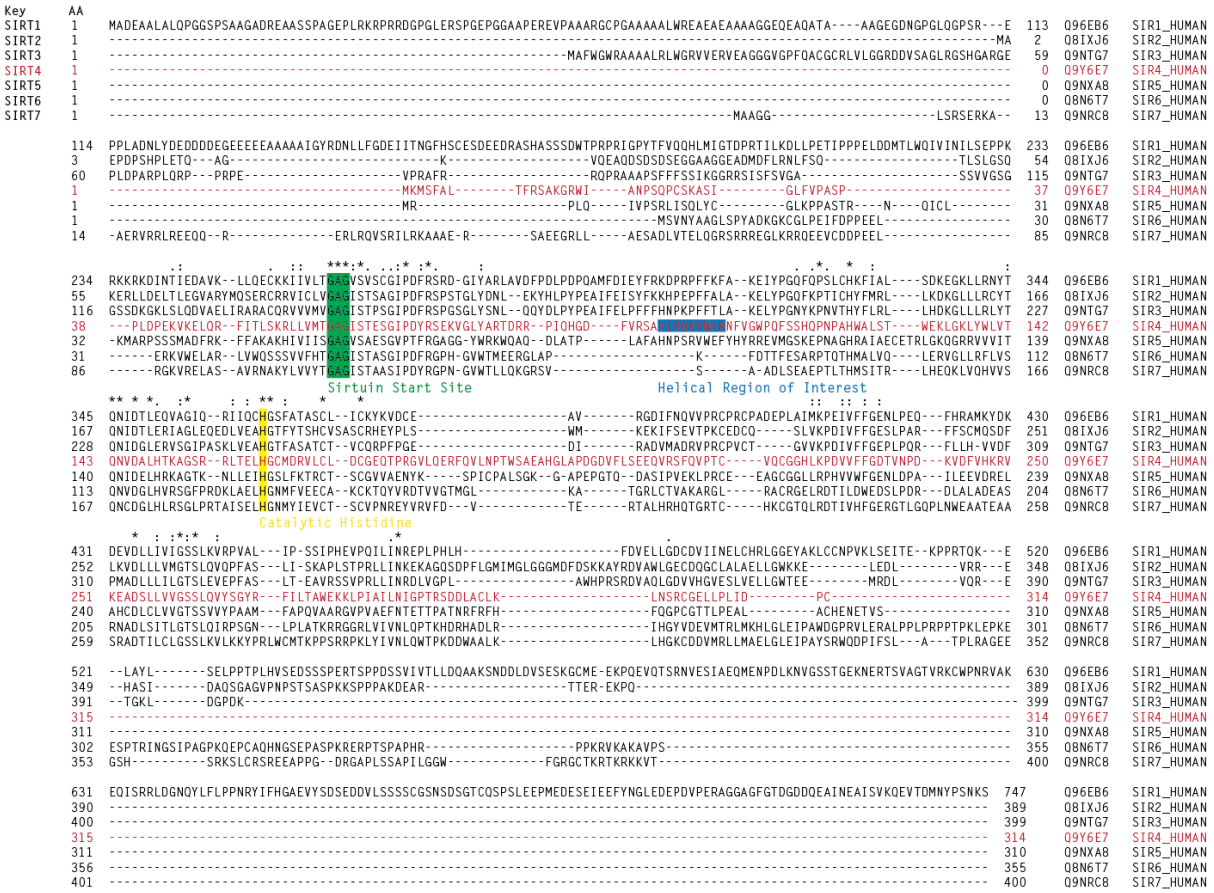

Figure S1 (Related to Figure 1)
(A) Uniprot sequence alignment of human sirtuins 1-7 using the identifiers: Q96EB6, Q8IXJ6, Q9NTG7, Q9Y6E7, Q9NXA8, Q8N6T7, Q9NRC8 for SIRT1-7, respectively.
(B) Newick format file representing the tree constructed by FastTree from all sirtuin sequences assigned to the sirtuin PFAM domain (PF02146) longer than 40 amino acids; the names of internal nodes give the support for these nodes, available for download at https://figshare.com/s/e51648137c9a0314616e;
(C) Tree built from all sirtuin sequences of length greater than 40; this tree supports the classical grouping of the human sirtuins and highlights the existence of several other, mainly microbial sirtuin clusters, available for download at https://figshare.com/s/e51648137c9a0314616e;
(D) Specificity determining position scores obtained by applying the GroupSim algorithm to an alignment of 81 diverse sirtuins; several positions in the SIRT4 'RQRYWAR' sequence received high scores indicative of importance in distinguishing class II sirtuins from other classes, available for download at https://figshare.com/s/e51648137c9a0314616e.

	SIRT1	SIRT2	SIRT3	SIRT4	SIRT5	SIRT6	SIRT7
SIRT1							
SIRT2	36.94						
SIRT3	35.17	47.16					
SIRT4	24.46	26.07	26.98				
SIRT5	26.79	24.81	28.4	28.37			
SIRT6	20.74	25.17	26.85	28	20.72		
SIRT7	21.29	20.71	25.09	26.79	22.87	37.95	

Figure S2 (Related to Figure 2). Identity matrix of SIRT4 compared to other sirtuins; accessed from: http://www.ebi.ac.uk/Tools/services/rest/clustalo/result/clustalo-I20140522-174546-0317-16067290-es/pim

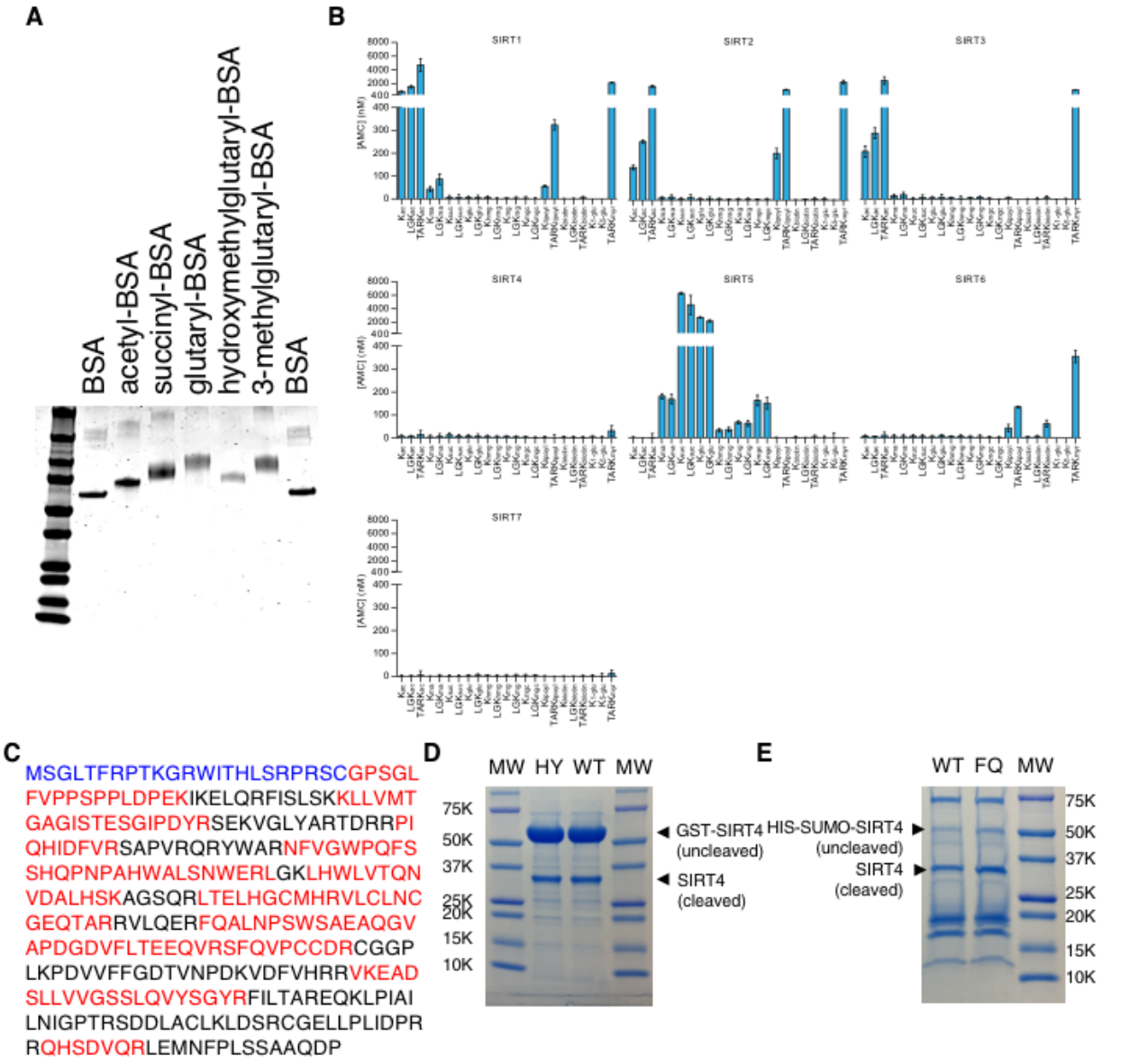

Figure S3 (Related to Figure 3).
(A) Coomassie-stained gel of BSA incubated with indicated anhydrides or CoA species; gel shift demonstrates successful acylation; 2 µg of each BSA on 4-16% SDS gel;
(B) Acylated lysine (K), leucine-glycine-lysine (LGK), or threonine-alanine-arginine-lysine (TARK) peptides with a fluorogenic 7-amino-4-methylcoumarin (AMC) probe were incubated with sirtuins SIRT1-SIRT7 obtained from commercial sources. Upon removal of the acyl group and trypsin treatment, the AMC fluorophore is released.
(C) Mass spectrometry results of mSIRT4 coverage; blue, mitochondrial targeting sequence (MTS); red, peptides identified after tryptic cleavage; raw data is in Supplementary Table 2.
(D) Representative gel showing recombinant GST-SIRT4 and GST-SIRT4HY fusion proteins were expressed in bacteria. The ~60 kDa GST-SIRT4 and -SIRT4HY fusion proteins (uncleaved) were then incubated with PreScission Protease to cleave off the GST-tag and release the ~33 kDa untagged SIRT4 proteins (cleaved). 4-20% acrylamide gel, 10 µg total protein loaded per lane, Stained with InstantBlue Coomassie stain,
(E) Representative gel showing recombinant His-SUMO-SIRT4 and His-SUMO-SIRT4FQ fusion proteins were expressed in bacteria. The ~50 kDa His-SUMO-SIRT4 and –SIRT4FQ fusion proteins (uncleaved) were then incubated with SUMO Protease to cleave off the His-SUMO-tag and release the ~33 kDa untagged SIRT4 proteins (cleaved); 4-20% acrylamide gel, 5 µg total protein loaded per lane, Stained with InstantBlue Coomassie stain.

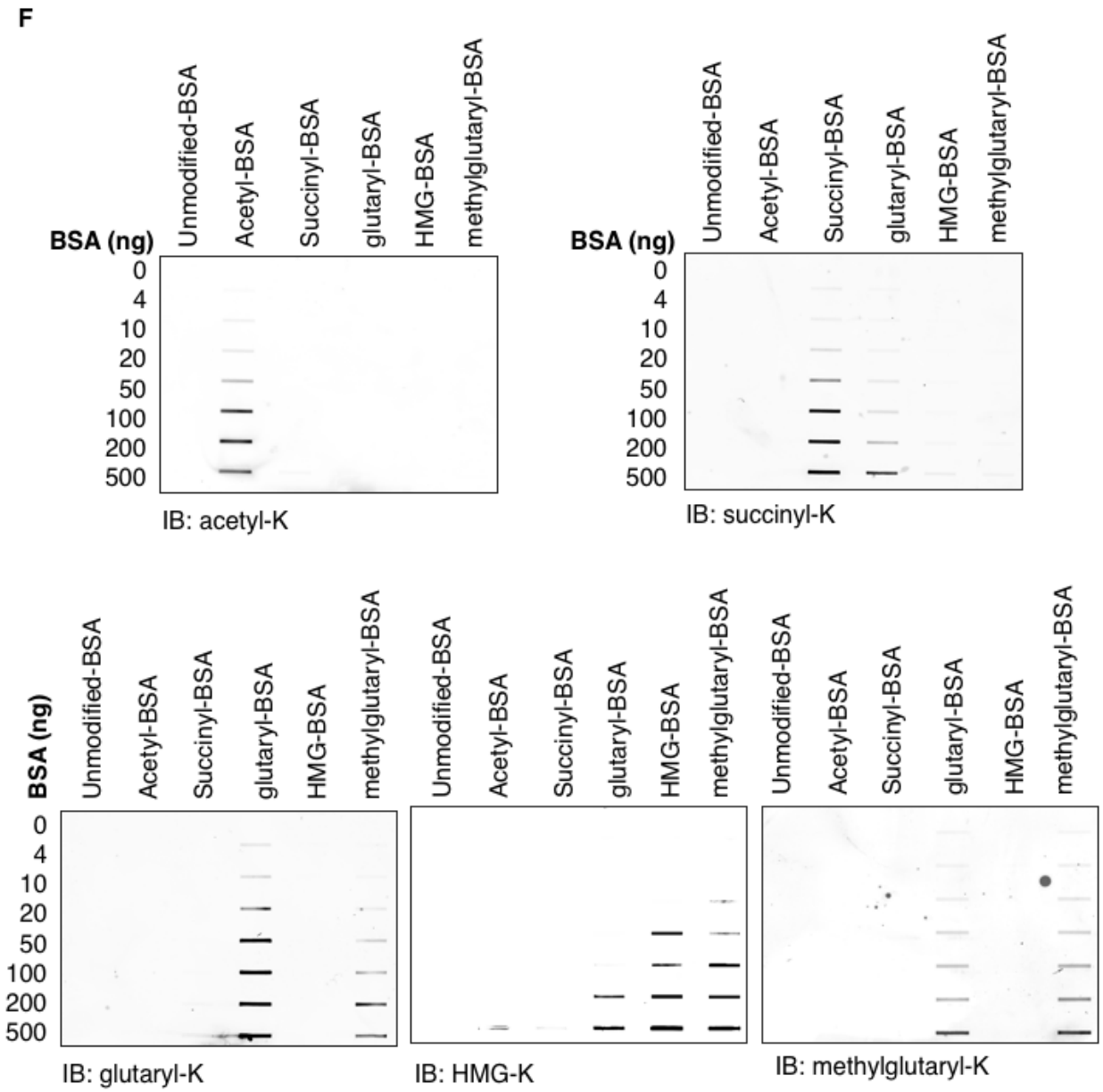

Figure S3 (Related to Figure 3), continued.
(F) Slot blots to evaluate cross-reactivity of acyl-K antibodies. A range of various acyl-BSAs (1-500 ng) were applied to each blot, then probed with indicated acyl-K antibodies.

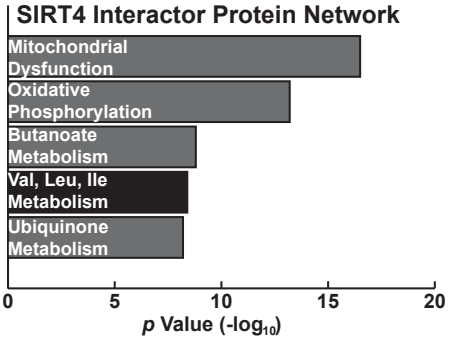

Figure S4 (Related to Figure 4). SIRT4 protein interaction network based on Ingenuity Pathway Analysis from bait-prey co-immunoprecipitation mass spectrometry experiments.

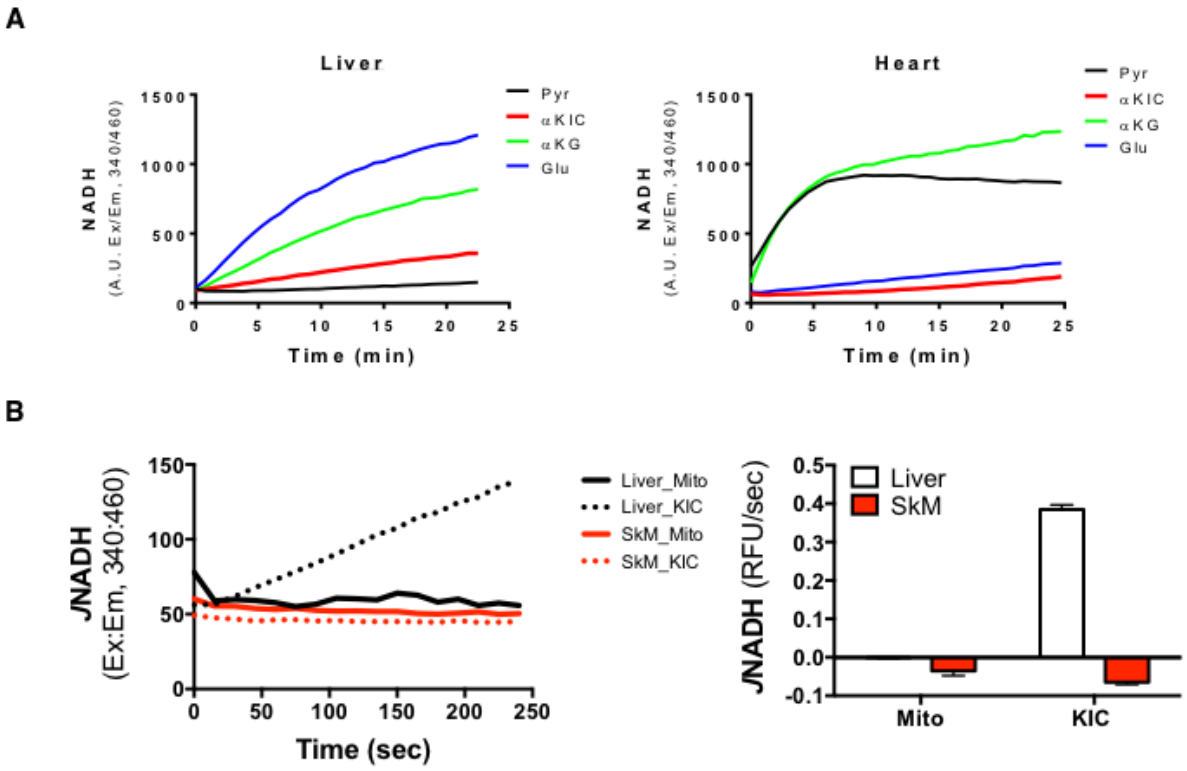

Figure S5 (Related to Figure 5).
(A) Representative trace of pyruvate (Pyr), α-ketoisocaproate (αKIC), α-ketoglutarate (αKG), and glutamate (Glu) flux measured *ex vivo* in WT and SIRT4KO male mouse liver mitochondria, monitored by NADH fluorescence (excitation 340nm/emission 460nm), representative of n=9/9, WT/SIRT4KO mice.
(B) Left: representative traces of basal (Mito) and KIC oxidization rates shown by NADH fluorescence in liver and skeletal muscle (SkM) in male wild-type mice. Right: Summary of rate of basal and KIC-stimulated oxidation; n=4/4.

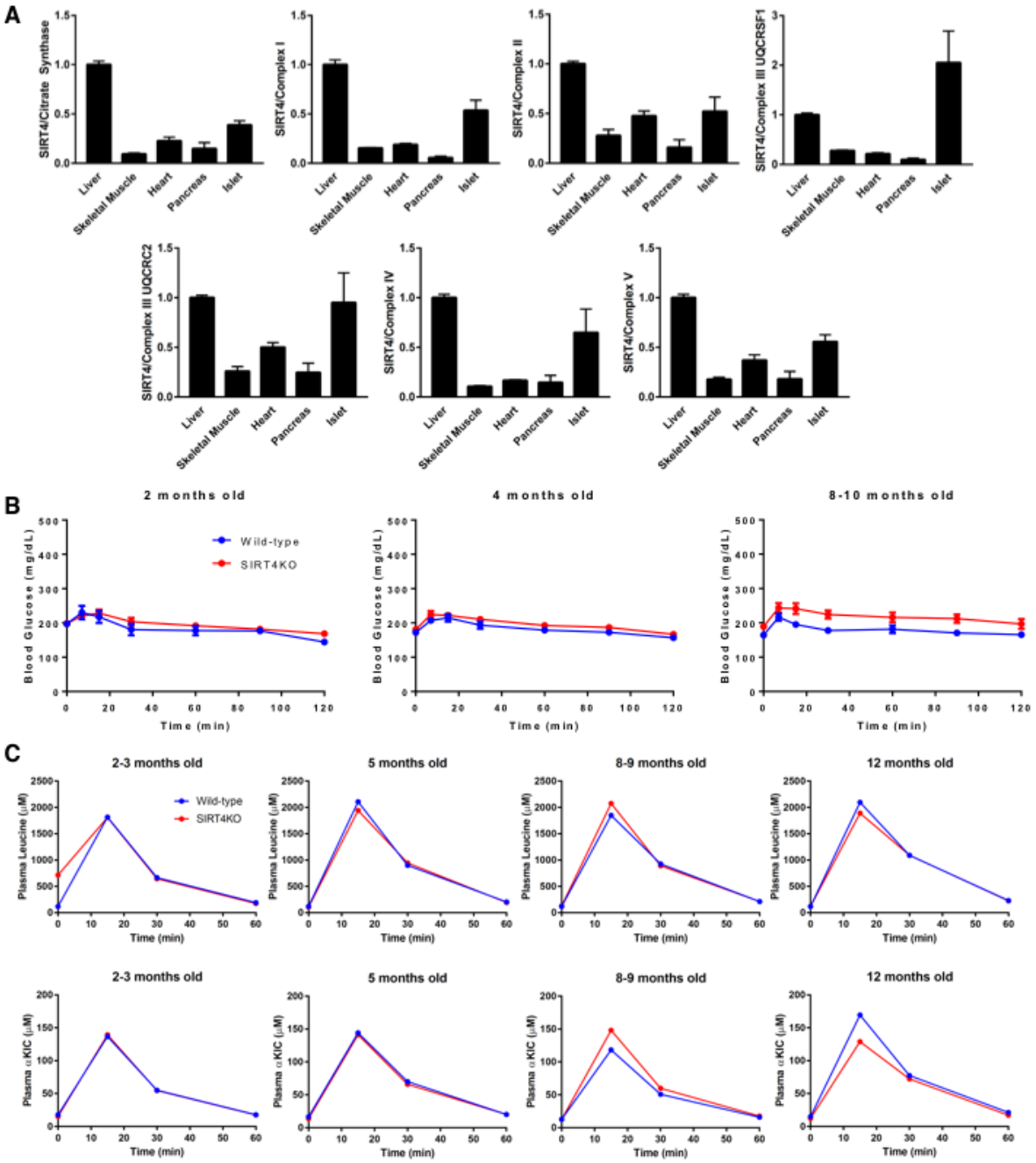

Figure S6 (Related to Figure 6).

(A) SIRT4 expression in liver, skeletal muscle (SKM), heart, pancreas, and pancreatic islets normalized to individual mitochondrial markers; citrate synthase (CS), complex I (CI), complex II (CII), complex III subunit 5, ubiquinol-cytochrome C reductase, Rieske iron-sulfur polypeptide 1 (CIII, UQCRFS1), complex III subunit 2, ubiquinol-cytochrome C reductase core protein II (CIII, UQCRC2), complex IV (CIV), complex V (CV).

(B) Blood glucose was measured in 2 month old (n=4/7 WT/SIRT4KO), 4 month old (n=15/15), and 8-10 month old (n=11/11) wild-type and SIRT4KO male mice following an oral gavage of 0.3 mg/g leucine.

(C) Plasma leucine and α-ketoisocaproate (αKIC) levels were measured by mass spectrometry in 2-3 month old (n=6/5 WT/SIRT4KO), 5 month old (n=6/4), 8-9 month old (n=5/4), and 12 month old (n=4/7) wild-type and SIRT4KO male mice following an oral gavage of 0.3 mg/g leucine. Plasma samples from each genotype at each time point were pooled to obtain enough plasma for reliable measurements by mass spectrometry.